Lab on a Chip

Cite this: *Lab Chip*, 2012, **12**, 3700–3706

www.rsc.org/loc

PAPER

A compact optofluidic cytometer with integrated liquid-core/PDMS-cladding waveguides†‡

Peng Fei,§[ab] Zitian Chen,§[ab] Yongfan Men,[ab] Ang Li,[ab] Yiran Shen[ac] and Yanyi Huang*[abc]

Received 5th April 2012, Accepted 9th May 2012
DOI: 10.1039/c2lc40329c

We developed a simple method to construct liquid-core/PDMS-cladding optical waveguides through pressurized filling of dead-ended micro-channels with optical fluids. The waveguides are in the same layer as microfluidic channels which greatly simplifies device fabrication. With proper contrast between the refractive index of the core and cladding, the transmission loss of the waveguides is less than 5 dB cm^{-1}. We also developed a method to create flat and optically clear surfaces on the sides of PDMS devices in order to couple light between free-space and the waveguides embedded inside the chip. With these newly developed techniques, we make a compact flow cytometer and demonstrate the fluorescence counting of single cells at a rate of up to $\sim$50 cell s^{-1} and total sample requirement of a few microlitres. This method of making liquid-core optical waveguides and flat surfaces has great potential to be integrated into many PDMS-based microsystems.

Introduction

Optofluidics, usually defined as the marriage of optics and fluidics,[1,2] takes advantage of the unique properties of liquid for the purpose of optical applications. The introduction of liquid into optical devices offers a simple mechanism to alternate the optical properties of the devices, smooth surfaces or interfaces between optical media, and dynamically reconfigure the shape of optical components. Many demonstrations of liquid-based optical components, including the liquid mirror for telescopes[3,4] and electro-wetting lenses,[5] have shown that liquid components can have advantages over their solid equivalents. Moreover, the fluids are highly flexible and adaptable, making them suitable for integration with miniaturized devices.[1,2,6,7] Many micro-optical components, such as ring resonatosr,[8,9] periodic photonic structures,[10,11] microlenses[12,13] and waveguides,[14] have been incorporated into chip-based devices. These integrations allows for various types of experiments including miniaturized imaging,[15–17] optical analysis and sensing.[18–21]

Flow cytometry is one example of the power of combining optics with fluidics. Flow cytometers have been widely used in clinical diagnosis and life science, to analyze, distinguish and count cells/particles suspended in fluid. This technique is naturally suitable to be implemented on optofluidic platforms with great reduction in device size and cost.[22,23] The first integration of flow cytometry into a microfluidic network was demonstrated by Eyal and Quake.[24] Afterward, the integration of optical waveguides or microlenses to precisely direct light to cell/particle samples and to collect the detection signals without misinterpretation has been demonstrated.[25–34]

Waveguides, with the ability to guide light with controllable confinement, are key components for chip-based cytometer devices. Traditional solid waveguides for lab-on-a-chip applications have been previously fabricated through multiple microfabrication methods, such as oxide deposition,[35] ion-exchange[36] and anisotropic etching of silicon.[37] Concurrently with the widely used soft-lithography technique, waveguides made of polymers such as PMMA, SU-8,[34,38] UV-laser-written optical adhesives[39] and poly(dimethylsiloxane) (PDMS)[40,41] have grown in popularity due to the low cost of these materials and the rapid fabrication processes.

Liquid waveguides, including liquid–liquid waveguides[14,42,43] and liquid core waveguides,[44–47] have been intrinsically integrated into the optofluidic platforms with large design flexibility. Through liquid waveguide components, many applications such as an interferometer sensor,[48] a waveguide dye laser,[49] and a pneumatically tunable laser[50] have also been realized. It is inconvenient however to integrate liquid core waveguides with alien solid claddings on optofluidic chips based on soft matters. On the other hand, most liquid–liquid waveguides are formed by continuous flow, which creates adjustable contrast of refractive index and the shape of certain optical components. The stability of the optical properties is usually determined by the stability of liquid flow, increasing the complexity of device control.

In this paper, we use a simple and robust method to integrate liquid core waveguides with dead ends into a monolithic PDMS

[a]*College of Engineering, Peking University, Beijing, 100871, China. E-mail: yanyi@pku.edu.cn*
[b]*Biodynamic Optical Imaging Center (BIOPIC), Peking University, Beijing, 100871, China*
[c]*College of Chemistry and Molecular Engineering, Peking University, Beijing, 100871, China*
† Published as part of a themed issue on optofluidics.
‡ Electronic supplementary information (ESI) available: Supporting figures. See DOI: 10.1039/c2lc40329c
§ These authors contributed eaqually to the work.

chip to build a compact cytometer. PDMS, as well as some other elastic polymers, is gas permeable. Therefore, a dead-ended channel can be filled by injecting liquid with external pressure, while expelling the air through the bulk PDMS. This method has been employed to build monolithic pneumatic valves,[51] to perform biochemical reactions[52] with pre-determined volumes, and to construct microlenses.[17] We create the static liquid core waveguide by injecting fluid with a refractive index slightly higher than PDMS into the empty dead-ended microchannels made by soft lithography. The waveguides, with a liquid core and PDMS cladding, can be designed into any geometry with predictable performance. A major advantage of this method is that all waveguides can be simply fabricated as microfluidic channels with other channels simultaneously through soft lithography.[29,44] With filling of specific optical fluids, some channels become waveguides and others can still be used for delivering samples or reagents. Compared to the approaches using solid waveguides or optical fibers, this method greatly reduces the fabrication complexity, as well as cost. In contrast to the previous reports, our method used non-volatile, liquid-core waveguides, which are stable for a long time because liquid flow is not necessary. We have also developed a simple method to form optically flat end-facets of the chip, allowing the light to be easily coupled into the waveguides. We have constructed a cytometer and collected fluorescence signals from cells flowing through a small excitation volume. Excitation and emission are both transmitted through multimode liquid-core waveguides. This low-cost and simple method of making optofluidic devices has great potential to be adapted to various biomedical and biophotonic applications.

Materials and methods

Device fabrication

The schematic of chip fabrication is shown in Fig. 1(a). Liquid PDMS was deposited on a mold made of positive relief patterns of SU-8 photoresist (MicroChem, Newton, MA, USA) on silicon wafers. After curing at 80 °C the PDMS negative (thickness ~2 mm) is peeled off the mold and inlet ports are punched in the device. The chip is then permanently bonded with a flat PDMS slab (thickness ~2 mm) using oxygen-plasma surface treatment, sealing the channels inside a monolithic piece. The dead-ended

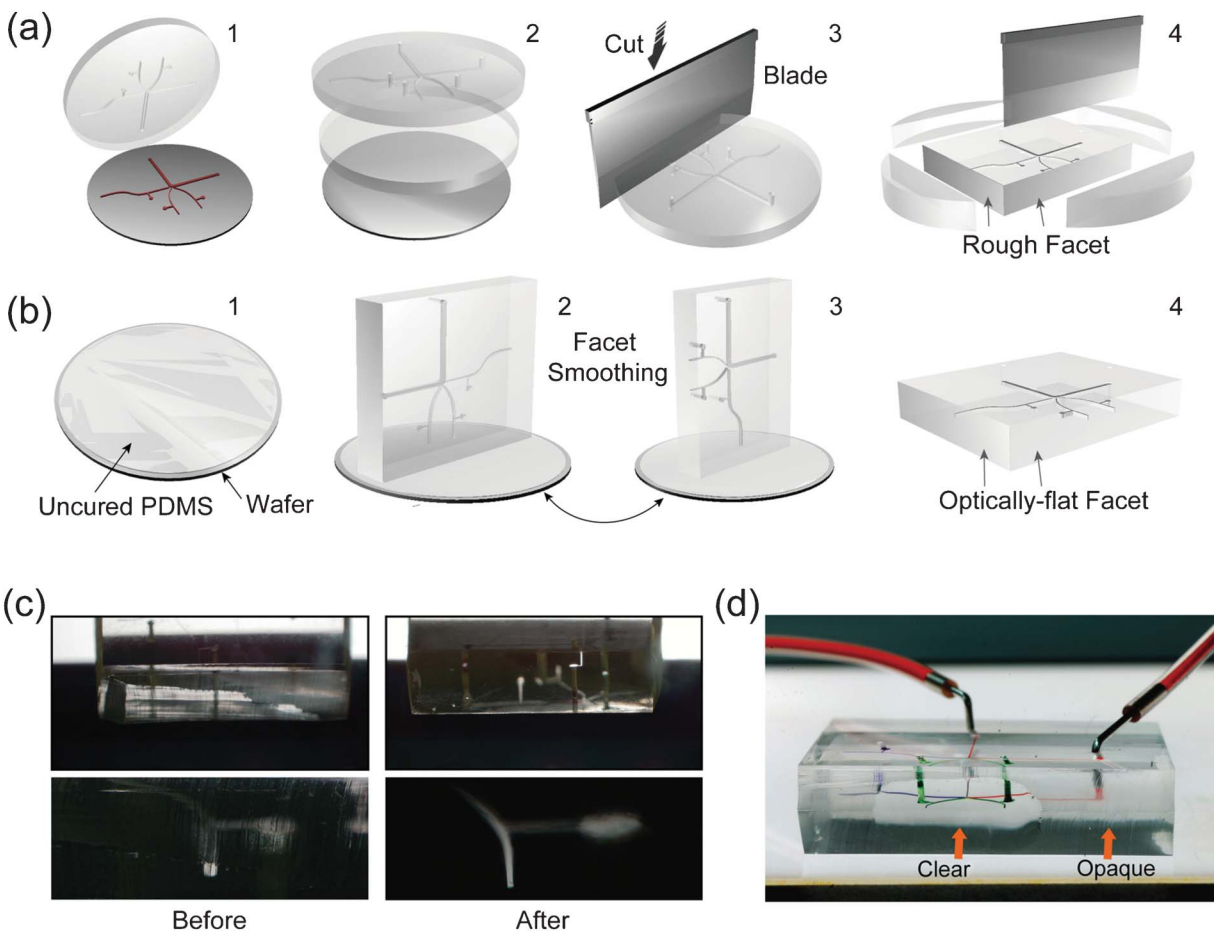

Fig. 1 Fabrication of the PDMS cytometer with integrated liquid-core waveguides. (a) Device fabrication. After the empty waveguides and fluid channels are formed and sealed into a monolithic PDMS piece (steps 1 & 2), we cut the chip into a rectangular shape (step 3) with rough facets (step 4). (b) Facet flattening. We prepared a thin layer of uncured PDMS on a Si wafer (step 1), and then vertically placed the chip on it (step 2 & 3). After curing, the chip was peeled off the wafer and exposed the optically-flat facets (step 4). (c) The contrast between the facet before and after the flattening process. (d) A completed cytometer chip with partially flattened facet. The smoothness of the optically-flat facet is critical to couple light in and out of the chip. Dye solutions are filled into the channels to indicate the optical waveguides and fluidic routes.

channels for waveguides are placed within the same layer as the microfluidic sample channels. We cut the PDMS slabs into rectangular chips using a razor blade in order to couple light in and out of the waveguides through the side facets of the devices. The position of the side surfaces is important. Usually we chose to cut the facet very close to the end of the channels for liquid waveguides, leaving <1 mm space in between. In that way, we would be able to use objective lenses or fibers with a short working distance to couple the light in and out of the waveguide. However, the freshly cut surfaces were rough with blade marks, making the light coupling inefficient due to the scattering loss.

To reduce this loss at the air–PDMS interface, we performed an additional step to make the optically-flat facets, shown in Fig. 1(b). We first spin-coated a thin layer (<500 μm) of uncured PDMS on a silicon wafer. Then we placed the PDMS chips with rough facets against the uncured PDMS, and cured at 80 °C for 30 min. After curing, we peeled the chip off the wafer and the end facets became optically clear and flat, as shown in Fig. 1(c) and (d).

Device structure

In order to make a cytometer chip, we designed three curved micro-channels with dead ends to be filled with liquid as optical waveguides (Fig. 2(a)). We filled these channels with high-quality immersion oil (Nikon Corporation) as the core medium with a slightly higher refractive index (n = 1.515) than the cladding material PDMS (n = 1.47). The liquid is injected under a pressure of 1×10^5 Pa, which is generated from an air compressor and is controlled by a regulator. We connect the inlets of the PDMS chip with liquid through microbore silicone tubing and stainless steel pins. The height of the channels is 60 μm. The width of the waveguide channels is 80 μm, and the width of the microfluidic sample channel is 80 μm. The geometries of these channels are highly configurable through design. After the immersion oil completely filled the dead-ended channels, we disconnected the oil supply from the chip and the waveguides were stable. The oil does not penetrate into the PDMS, nor does it evaporate. For each waveguide, the liquid was injected from the side of the channels (Fig. 2), ensuring the minimum loss of the light during propagation.

Optical coupling

The optical configuration of the experiment is shown in Fig. 2(b). A laser beam (473 nm, MBL50, Changchun optoelectronics, peak power 50 mW) is coupled into the excitation waveguide through an objective (32×, Leitz, NA 0.60). The fluorescence signals and the back-scattering of excitation are collected and guided through two other curved waveguides and then coupled into another objective (4×, Nikon, NA 0.13). The fluorescence signal is filtered by a fluorescence microscope (Eclipse TE2000-S, Nikon), and then detected by an EMCCD (iXon DU-897D, Andor Technology).

Preparation of single cell suspension

We centrifuged the U2OS cell suspension using a 1.5 ml centrifugal tube, and then replaced the medium with Ca/Mg-free PBS buffer without phenol red to minimize background

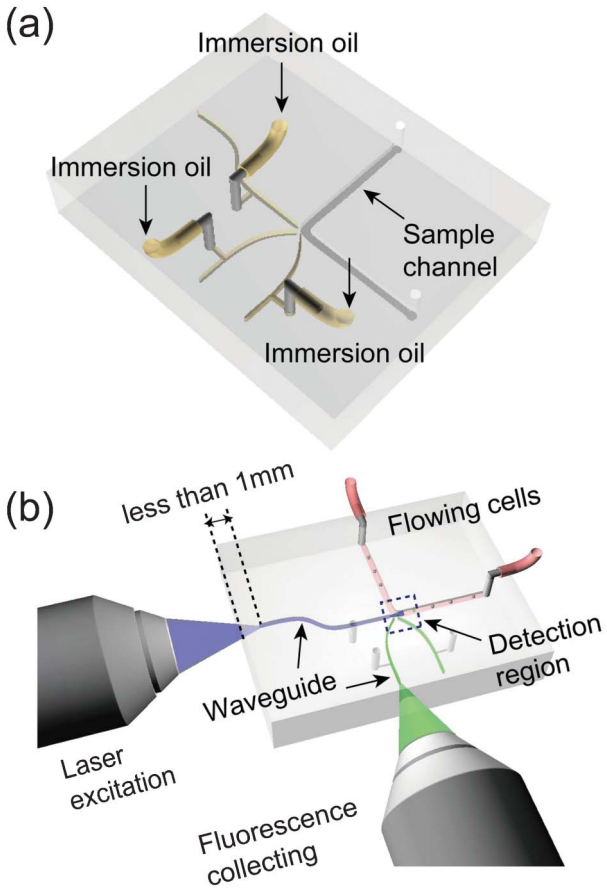

Fig. 2 Structure of a cytometer chip. (a) Components of the device. The curved dead-ended channels (yellow) are completely filled with immersion oil with refractive index n = 1.515. The sample (red), such as a single cell suspension, is introduced into the L shaped microfluidic channel. (b) Optical configuration of the cytometer. A focused laser beam is coupled into the excitation liquid-core waveguide (blue) through an objective. The fluorescence signal generated from the cells or particles is guided through the collection waveguides (green), and then coupled out of the chip through another objective.

fluorescence. We stained the cells with 0.2 mg ml^{-1} calcein-AM for 40 min, and then centrifuged the suspension and transferred the cells to PBS-based single cell buffer containing 0.1% BSA, 1 mM EDTA, 25 μg ml^{-1} DNAse I and 1 mM $MgCl_2$. Before the experiment, we use a nylon mesh to remove the remaining clumps in the suspension. The final density of the suspension is 1×10^5 to 1×10^6 cells ml^{-1}.

Results and discussion

One of the major challenges of optofluidic integration is finding an efficient method to deliver light in and out of the chip. Integrating pig-tailed fibers can provide a simple solution to this issue, but it comes with higher cost of fabrication and less flexibility of the device. For our devices, we used objectives to couple light between free-space and the waveguides embedded inside the chip. This method can be combined with various optical setups for imaging or spectral studies. The flatness of the chip's side surfaces is a critical factor for coupling. It is commonly observed that the side surfaces of PDMS chips cut by

razor blades are intrinsically scattering because the blade marks on the surface make it an optical diffuser. Unlike devices made from glass, this surface cannot be easily polished. One technique reported a low-loss side surface made from glass that increased the coupling efficiency.[44] Our method used full PDMS to create optically-flat surfaces with high light coupling efficiency. This flattening procedure is also a powerful tool to observe the side view of the internal structure inside a PDMS based microfluidic device.

A 473 nm semiconductor laser was used for exciting the calcein-AM stained cells to generate green emission. The laser power was adjusted by a variable neutral density (ND) filter. We used a three-dimensional translational stage to finely tune the beam focus and to couple into the tip of the waveguides. The experimental setup is shown in Fig. S1.‡ The alignment is critical, as shown in Fig. 3(a). The cross section of the excitation waveguide is 80 × 60 μm, allowing easy coupling from free space using a 32× objective with NA 0.60. Maximum coupling efficiency is only achieved when the laser focus is well aligned with the entrance of the waveguide. The confined laser propagates along the waveguide channel and finally emerges from the other end. The end of the waveguide is designed to be very close to the sample channel, ensuring that only a small region of the channel is excited. To further eliminate the background induced by the laser that propagated outside of the waveguide, we designed the excitation waveguide to be an "S" shape. The sample channel was designed to be an "L" shape, with the corner close to ends of three waveguides (Fig. 3(b)). Once the liquid-core waveguides are formed, the only physical world-to-chip interface is the sample introduction. No further actions are needed to maintain the waveguiding functions. The optical loss of these liquid-core waveguides are measured to be ~5 dB cm^{-1}, which is acceptable for most bio-sensing applications.

Two detection waveguides are closely aligned to the corner. Due to the limited numerical aperture (NA) of around 0.4 and acceptance angle of around 50 degrees, only the induced fluorescence from the cells very close to the detection waveguides can be efficiently collected. On the other hand, coupling of the scattered laser is greatly suppressed. Therefore, the excitation

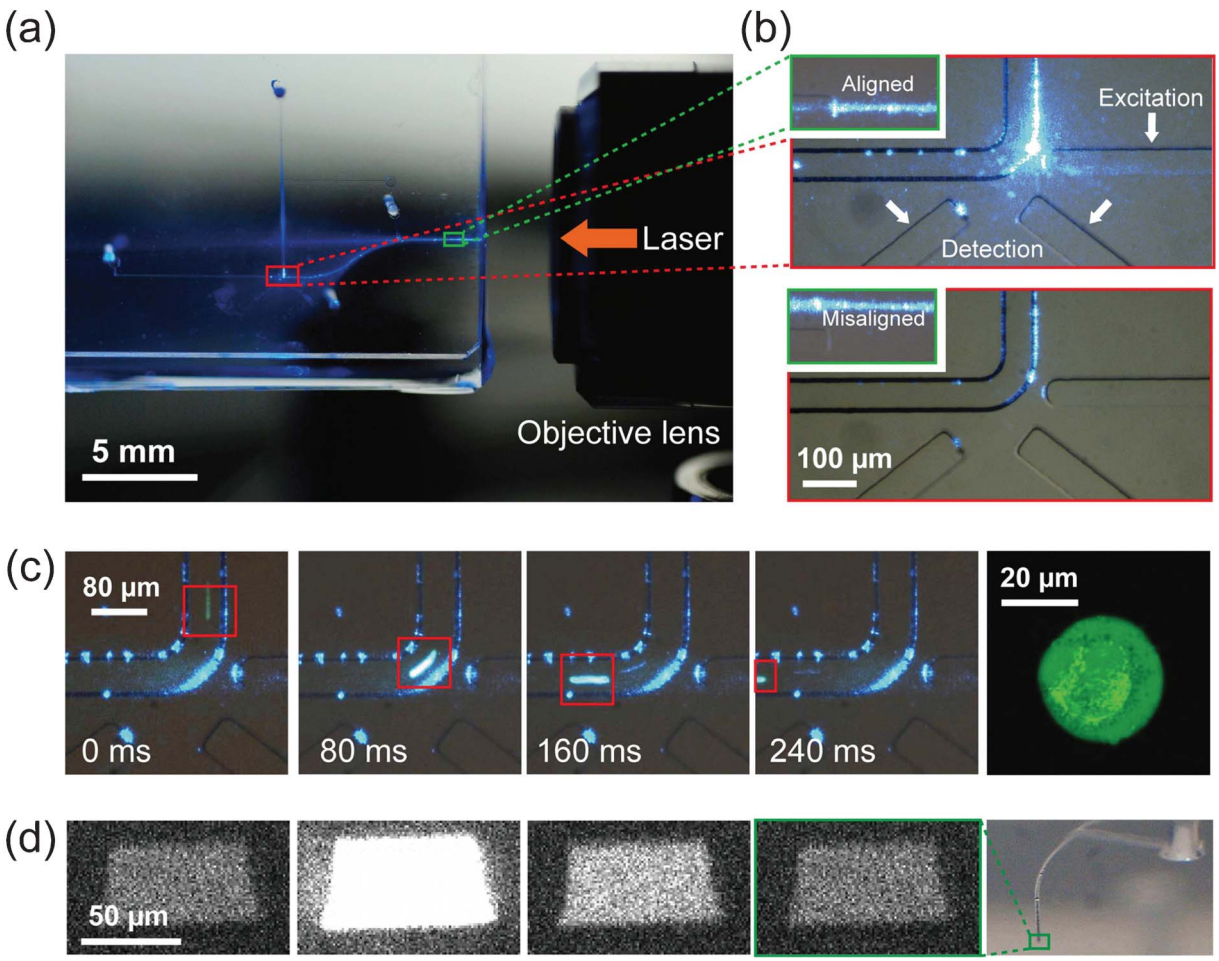

Fig. 3 Detecting fluorescently labeled single cells with liquid-core waveguides. (a) A cytometer chip with an objective to couple 473 nm laser light into the excitation waveguide. Laser light is guided along a curved waveguide. (b) Microphotographs of the detection region. When the laser is properly coupled into the excitation waveguide, the detection region is strongly illuminated. (c) The microphotographs of a fluorescently labeled U2OS cell passing through the detection region at a relatively low speed (~1.5 mm s^{-1}). The right panel is a confocal image of individual living cells stained with calcein-AM. (d) The EMCCD images of the output end-facet of the detection waveguide, corresponding to the top-views in (c). The right panel is a microphotograph of a detection waveguide observed from the optically flat side surface of the chip.

waveguide together with the detection waveguides define an effective detection region at the channel corner, with an approximate length less than 300 μm. Both detection waveguides could efficiently collect the signals. We typically fabricated two waveguides for signal collections and used one of them during the experiments. The detection volume is ~1 nL. The suspension of living cells, stained with calcein-AM, is introduced into the sample channels using a syringe pump with a typical flow rate of 100–300 μl h^{-1}. When each single cell flows through the detection region, it will be excited by the laser and emit bright fluorescence peaked at 510 nm. We placed another ultra-long working-distance objective (5×) and a CCD video camera (QHY-IMG 2S, 25 fps) to monitor the whole process from the top. Fig. 3(c) shows the time-lapse frames of a single cell passing through the detection region at a low speed of 1.5 mm s^{-1}. Each flowing cell in this region is intensively excited and emits fluorescence with varying intensities that are strongly related to the cell location. In the detection region, the cell's fluorescence is mostly collected by the detection waveguides and propagates towards the waveguide's end facet. We employed an inverted microscope with an EMCCD to observe the fluorescence signal coupled from the detection waveguides. To achieve a high signal to noise ratio, we used a filter cube to further block the scattered laser signal. The EMCCD can capture the images of the end facet of the detection waveguide. Fig. 3(d) shows the brightness variation at different time points, which matches the observation from the top approximately. We converted these time-lapse images into intensity traces with time for analyzing flow velocity or counting cells or particles.

To count the single cells at higher flowing velocity, we further increase the imaging frame rate by reducing the exposure time and frame size of each image. An electron multiplying level of 300 and a small range of interest (512 × 10 pixels, the smaller dimension was in the frame-shift direction of the CCD sensor) were used to shorten the exposure time to 1 ms. Using this configuration, the frame rate can be greatly boosted to a limit of 400 fps.

We tested the counting performance of our chip-based optofluidic cytometer by adjusting the flow speed of the cell suspension. When the density of cells is 2 × 10^5 ml^{-1} and the flow rate is 200 μl h^{-1}, the velocity of the single cells is relatively low and we can capture every single-cell events with 512 × 60 pixels images at 100 fps (Fig. 4(a), panel 1). The flow trace can be easily exacted from the sequential images by picking one slice of each image (60 × 1 pixels) and stitching them together, as shown in Fig. 4(a), panel 2. The bright stripes represent single-cell events when the fluorescently labeled cells pass the detection region. Detailed images and intensity trace (Fig. 4(a), panel 3, and Fig. 4(b)) show that most of the single-cell events can be clearly identified with a very small false negative count rate. We used a predetermined threshold to differentiate the fluorescence signal from the false counts. The reason lies in the fact that the

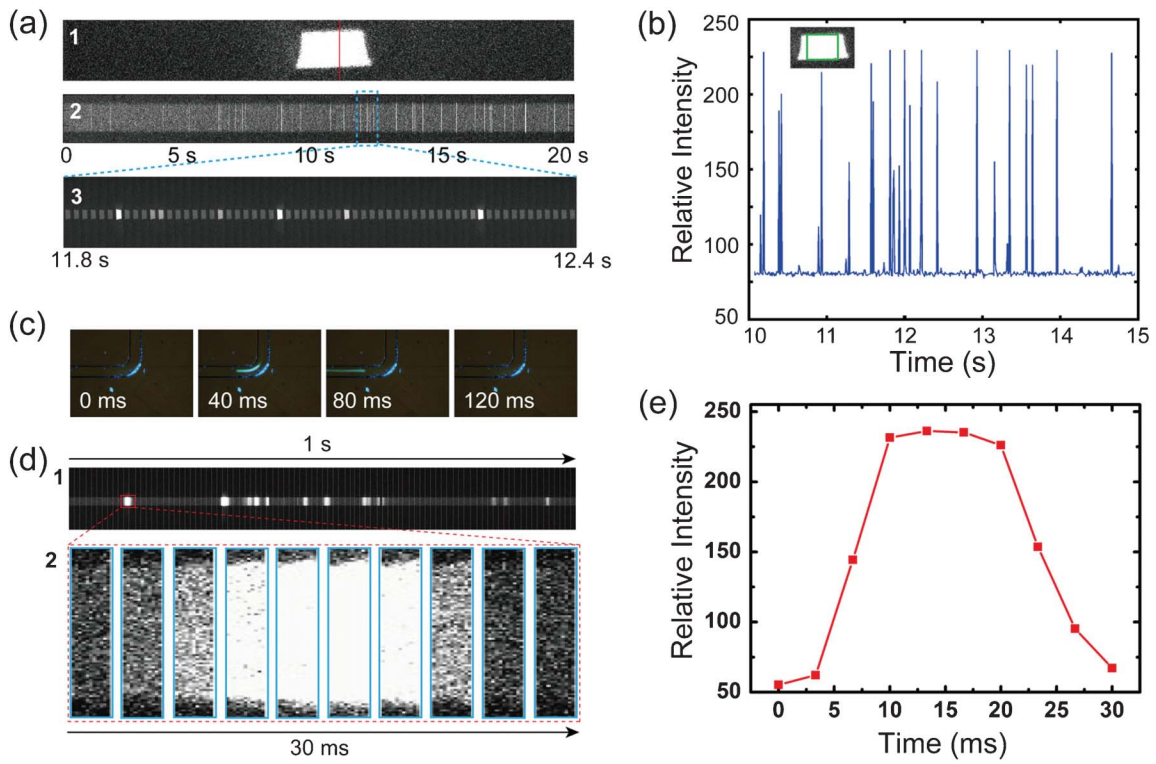

Fig. 4 Acquiring the fluorescence signal and counting the flowing cells with our cytometer device. (a) 2000 sequential fluorescence images (512 × 60 pixels) are taken at a frame rate of 100 fps (panel 1). We crop an ROI of 60 × 1 pixels (red line) from each image in the sequence, and align the cropped images into a panorama (panel 2). 60 frames are picked out to demonstrate the individual counts within 0.6 s (panel 3). (b) The intensity trace of the end-facet of the detection waveguide in 5 s, corresponding to the sequential images in (a). (c) The top-views of the single cells flowing through the detection region with speed at around 18 mm s^{-1}. (d) The sequential EMCCD images of the fluorescence signals guided through the liquid-core detection waveguide. The images are acquired at a frame rate of 380 fps for capturing the flowing single cells with high velocity. (e) The intensity trace of a single cell passing through the detection region.

sampling rate is not high enough to clearly discern two cells with an ultra-short spatial distance. Therefore, with the higher density of the cell suspension, $\sim 10^6$ ml^{-1}, and higher flow speed at 300 μl h^{-1}, we further increased the speed of image acquisition to 380 fps for accurately counting the single-cell events, as shown in Fig. 4(c) and (d). A typical single cell with a strong fluorescence signal will present as a distinct peak with full width at half maximum (FWHM) $\sim$10 ms in the trace, indicating that under this condition, our system is able to differentiate the single-cell events up to $\sim$50 cell s^{-1}. The total volume required for the detection can be as small as a few microlitres. The counting rate, which was limited by the EMCCD frame rate in the current setup, can be further improved using a highly sensitive photo detector and high-speed signal acquisition devices. Using photomultiplier tubes as the detector, we envision that this method has potential to count and sort the cells at the rate of 10^2–10^3 cells s^{-1}, which is comparable to most other approaches.[22]

Conclusions

In summary, we have developed a new method to easily integrate liquid-core optical waveguides into PDMS-based microfluidic devices. This method contains two innovations: (1) liquid waveguides formed in-layer with microfluidic channels and (2) optically-flat side surfaces of a PDMS device for optimized optical coupling. This method introduces many advantages into optofluidic devices. First, the waveguide structure is formed simultaneously with the fabrication of microfluidic channels, eliminating the complex fabrication procedure that is normally required for the integration of solid waveguides or optical fiber. Second, the waveguide creation by dead-end filling is simple and robust, greatly simplifying the device control. Third, the side surfaces of the chip can be simply smoothed into optically-flat surfaces with great optical throughput, which can be applied to any applications that require the optical coupling or observation through the side of the devices. Fourth, these oil-filled liquid-core waveguides have long-term stability, allowing for use as low-cost optofluidic devices in disposable bio-sensing applications with minimum requirement of external apparatus.

We demonstrated a compact flow cytometer with liquid-core waveguides and flattened PDMS side surfaces. With the waveguide-confined detection region at the nanolitre scale, we detected single cell events at up to 50 cell s^{-1} with merely a few microlitres of sample flowing inside the microfluidic channel. We envision this method can be widely integrated into many applications that combine optoelectronics with microfluidics, especially in bio-sensing, clinical diagnostics, point-of-care testing, and single cell analysis.

Acknowledgements

The authors thank Dr Aaron Streets, Zi He, Zhilong Yu, Chunhong Zheng, Yusi Fu and Xiannian Zhang for their fruitful discussion. Funding for this work was kindly provided by the National Natural Science Foundation of China (20890020, 90913011), the Ministry of Science and Technology of China (2011CB809106), and the Fok Ying Tung Education Foundation.

References

1 D. Psaltis, S. R. Quake and C. Yang, *Nature*, 2006, **442**, 381–386.
2 H. Schmidt and A. R. Hawkins, *Nat. Photonics*, 2011, **5**, 598–604.
3 E. F. Borra, *J. Royal Astron. Soc. Canada*, 1982, **76**, 245–256.
4 E. F. Borra, O. Seddiki, R. Angel, D. Eisenstein, P. Hickson, K. R. Seddon and S. P. Worden, *Nature*, 2007, **447**, 979–981.
5 S. Kuiper and B. Hendriks, *Appl. Phys. Lett.*, 2004, **85**, 1128.
6 C. Monat, P. Domachuk and B. J. Eggleton, *Nat. Photonics*, 2007, **1**, 106–114.
7 X. Fan and I. M. White, *Nat. Photonics*, 2011, **5**, 591–597.
8 I. M. White, H. Oveys and X. Fan, *Opt. Lett.*, 2006, **31**, 1319–1321.
9 U. Levy, K. Campbell, A. Groisman, S. Mookherjea and Y. Fainman, *Appl. Phys. Lett.*, 2006, **88**, 111107.
10 E. Chow, A. Grot, L. Mirkarimi, M. Sigalas and G. Girolami, *Opt. Lett.*, 2004, **29**, 1093–1095.
11 L. Rindorf, J. B. Jensen, M. Dufva, L. H. Pedersen, P. E. Hoiby and O. Bang, *Opt. Express*, 2006, **14**, 8224–8231.
12 N. Chronis, G. L. Liu, K. H. Jeong and L. P. Lee, *Opt. Express*, 2003, **11**, 2370–2378.
13 X. Mao, J. R. Waldeisen, B. K. Juluri and T. J. Huang, *Lab Chip*, 2007, **7**, 1303–1308.
14 D. B. Wolfe, R. S. Conroy, P. Garstecki, B. T. Mayers, M. A. Fischbach, K. E. Paul, M. Prentiss and G. M. Whitesides, *Proc. Natl. Acad. Sci. U. S. A.*, 2004, **101**, 12434–12438.
15 X. Q. Cui, L. M. Lee, X. Heng, W. W. Zhong, P. W. Sternberg, D. Psaltis and C. Yang, *Proc. Natl. Acad. Sci. U. S. A.*, 2008, **105**, 10670–10675.
16 G. Zheng, S. A. Lee, Y. Antebi, M. B. Elowitz and C. Yang, *Proc. Natl. Acad. Sci. U. S. A.*, 2011, **108**, 16889–16894.
17 P. Fei, Z. He, C. Zheng, T. Chen, Y. Men and Y. Huang, *Lab Chip*, 2011, **11**, 2835–2841.
18 P. Schwille, F. J. Meyer-Almes and R. Rigler, *Biophys. J.*, 1997, **72**, 1878–1886.
19 C. A. Barrios, M. J. Bañuls, V. González-Pedro, K. B. Gylfason, B. Sánchez, A. Griol, A. Maquieira, H. Sohlström, M. Holgado and R. Casquel, *Opt. Lett.*, 2008, **33**, 708–710.
20 W. Song, X. Zhang, A. Liu, C. Lim, P. Yap and H. M. M. Hosseini, *Appl. Phys. Lett.*, 2006, **89**, 203901.
21 W. Song and D. Psaltis, *Biomicrofluidics*, 2011, **5**, 044110.
22 S. H. Cho, J. M. Godin, C. H. Chen, W. Qiao, H. Lee and Y. H. Lo, *Biomicrofluidics*, 2010, **4**, 043001.
23 D. A. Ateya, J. S. Erickson, P. B. Howell, L. R. Hilliard, J. P. Golden and F. S. Ligler, *Anal. Bioanal. Chem.*, 2008, **391**, 1485–1498.
24 S. Eyal and S. R. Quake, *Electrophoresis*, 2002, **23**, 2653–2657.
25 D. Barat, G. Benazzi, M. C. Mowlem, J. M. Ruano and H. Morgan, *Opt. Commun.*, 2010, **283**, 1987–1992.
26 D. Huh, W. Gu, Y. Kamotani, J. B. Grotberg and S. Takayama, *Physiol. Meas.*, 2005, **26**, R73–R98.
27 J. P. Golden, J. S. Kim, J. S. Erickson, L. R. Hilliard, P. B. Howell, G. P. Anderson, M. Nasir and F. S. Ligler, *Lab Chip*, 2009, **9**, 1942–1950.
28 S. H. Cho, C. H. Chen, F. S. Tsai, J. M. Godin and Y. H. Lo, *Lab Chip*, 2010, **10**, 1567–1573.
29 S. H. Cho, W. Qiao, F. S. Tsai, K. Yamashita and Y. H. Lo, *Appl. Phys. Lett.*, 2010, **97**, 093704.
30 J. Godin and Y. H. Lo, *Biomed. Opt. Express*, 2010, **1**, 1472–1479.
31 M. Rosenauer, W. Buchegger, I. Finoulst, P. Verhaert and M. Vellekoop, *Microfluid. Nanofluid.*, 2011, 1–11.
32 C. Song, T. D. Luong, T. F. Kong, N. T. Nguyen and A. K. Asundi, *Opt. Lett.*, 2011, **36**, 657–659.
33 M. L. Chabinyc, D. T. Chiu, J. C. McDonald, A. D. Stroock, J. F. Christian, A. M. Karger and G. M. Whitesides, *Anal. Chem.*, 2001, **73**, 4491–4498.
34 G. B. Lee, C. H. Lin and G. L. Chang, *Sens. Actuators, A*, 2003, **103**, 165–170.
35 K. B. Mogensen, N. J. Petersen, J. Hübner and J. P. Kutter, *Electrophoresis*, 2001, **22**, 3930–3938.
36 S. Gaugiran, S. Gétin, J. Fedeli, G. Colas, A. Fuchs, F. Chatelain and J. Derouard, *Opt. Express*, 2005, **13**, 6956–6963.
37 K. K. Lee, D. R. Lim, L. C. Kimerling, J. Shin and F. Cerrina, *Opt. Lett.*, 2001, **26**, 1888–1890.
38 B. Bilenberg, T. Nielsen, B. Clausen and A. Kristensen, *J. Micromech. Microeng.*, 2004, **14**, 814.
39 K. S. Lee, H. L. T. Lee and R. J. Ram, *Lab Chip*, 2007, **7**, 1539–1545.
40 D. A. Chang-Yen, R. K. Eich and B. K. Gale, *J. Lightwave Technol.*, 2005, **23**, 2088.

41 C. L. Bliss, J. N. McMullin and C. J. Backhouse, *Lab Chip*, 2007, **7**, 1280–1287.
42 S. K. Y. Tang, B. T. Mayers, D. V. Vezenov and G. M. Whitesides, *Appl. Phys. Lett.*, 2006, **88**, 061112.
43 Y. Yang, A. Liu, L. Chin, X. Zhang, D. Tsai, C. Lin, C. Lu, G. Wang and N. Zheludev, *Nat. Commun.*, 2012, **3**, 651.
44 O. J. A. Schueller, X. M. Zhao, G. M. Whitesides, S. P. Smith and M. Prentiss, *Adv. Mater.*, 1999, **11**, 37–41.
45 S. H. Cho, J. Godin and Y. H. Lo, *IEEE Photonics Technol. Lett.*, 2009, **21**, 1057–1059.
46 S. L. Wang, X. J. Huang, Z. L. Fang and P. K. Dasgupta, *Anal. Chem.*, 2001, **73**, 4545–4549.
47 N. Gopalakrishnan, K. S. Sagar, M. B. Christiansen, M. E. Vigild, S. Ndoni and A. Kristensen, *Opt. Express*, 2010, **18**, 12903–12908.
48 R. Bernini, G. Testa, L. Zeni and P. M. Sarro, *Appl. Phys. Lett.*, 2008, **93**, 011106.
49 Y. Yang, A. Liu, L. Lei, L. Chin, C. Ohl, Q. Wang and H. Yoon, *Lab Chip*, 2011, **11**, 3182–3187.
50 W. Song and D. Psaltis, *Appl. Phys. Lett.*, 2010, **96**, 081101.
51 M. A. Unger, H. P. Chou, T. Thorsen, A. Scherer and S. R. Quake, *Science*, 2000, **288**, 113–116.
52 Y. Marcy, C. Ouverney, E. M. Bik, T. Lösekann, N. Ivanova, H. G. Martin, E. Szeto, D. Platt, P. Hugenholtz and D. A. Relman, *Proc. Natl. Acad. Sci. U. S. A.*, 2007, **104**, 11889–11894.

Electronic Supplementary Material (ESI) for Lab on a Chip

Supporting Information

An Ultracompact Optofluidic Cytometer with Integrated Oil-core/PDMS-cladding Waveguides

Peng Fei,§[a,b] Zitian Chen,§[a,b] Yongfan Men,[a,b] Ang Li,[a,b] Yiran Shen,[a,c] and Yanyi Huang*[a,b,c]

[a] *College of Engineering, Peking University, Beijing 100871, China. E-mail: yanyi@pku.edu.cn*

[b] *Biodynamic Optical Imaging Center (BIOPIC), Peking University, Beijing 100871, China*

[c] *College of Chemistry and Molecular Engineering, Peking University, Beijing 100871, China*

1. Supporting Figures

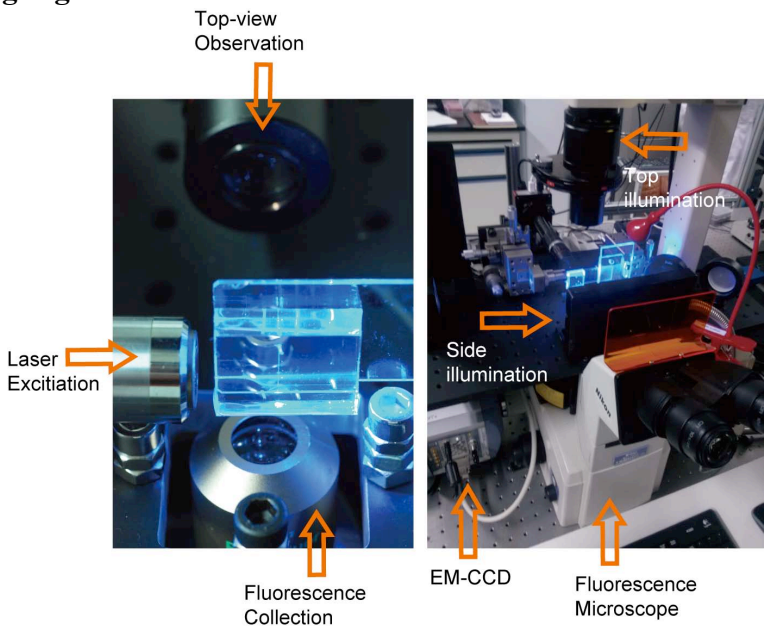

Fig. S1 The homebuilt apparatus for performance test of the cytometer chip. We machined an optical breadboard and mount it on a Nikon inverted fluorescence microscope. The semiconductor CW laser, sample holder, and objective for excitation are mounted on this breadboard with wide and precise tunability. We also built a horizontal imaging system containing a long working-distance objective lens and a CCD camera to provide the "top-view" observation of the device. Two imaging systems are integrated together to monitor the dynamic process and to count the cells simultaneously.

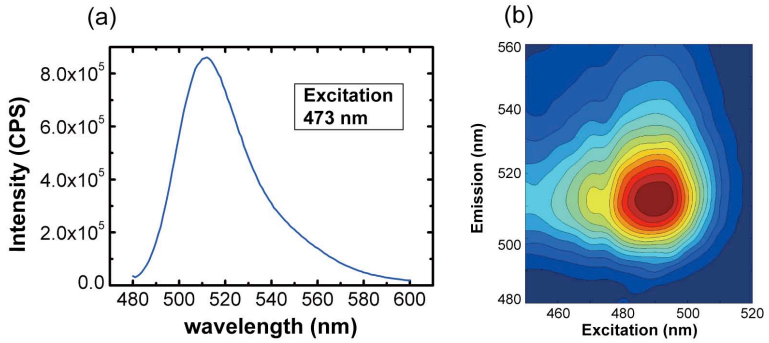

Fig. S2 The fluorescence spectrum of the suspension of live cells stained with calcein-AM. (a) The emission spectrum of the cell under 473nm excitation. (b) The two-dimensional spectrum revealing the relationship between the excitation and emission.

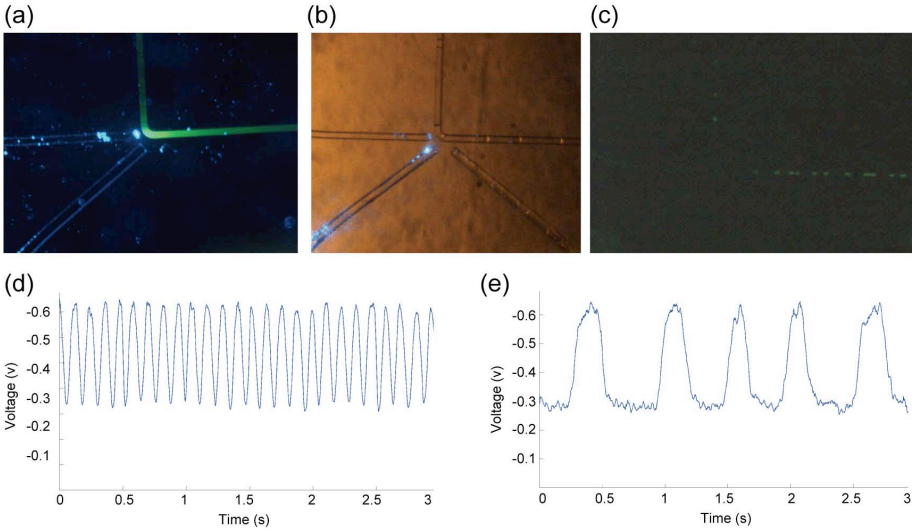

Fig. S3 Counting the fluorescence of the micro-droplet emulsions. (a) The precisely guided excitation causes a laser induced fluorescence (LIF) at a localized region. (b) The bright field image of the chip. The fluorescence aqueous droplets are formed in a stream of water-immiscible fluorinated carrier fluid. The droplets are separated by the carrier fluid and flow through the sensor region one by one. The size, velocity, and fluorescein concentration of the droplets can be changed easily. (c) The fluorescence image of the aqueous droplets. (d) and (e) show the counting result of the droplets with different size and velocity. Besides counting, we can also assess the size of the droplets from the plots.